HHS Public Access

Author manuscript

Chem. Author manuscript; available in PMC 2021 June 11.

Published in final edited form as:

Chem. 2020 June 11; 6(6): 1408–1419. doi:10.1016/j.chempr.2020.03.004.

Mitochondrial relocation of a common synthetic antibiotic: A non-genotoxic approach to cancer therapy

Kyoung Sunwoo[1,5], **Miae Won**[1,5], **Kyung-Phil Ko**[2], **Miri Choi**[4], **Jonathan F. Arambula**[3], **Sung-Gil Chi**[2,*], **Jonathan L. Sessler**[3,7,*], **Peter Verwilst**[1,6,*], **Jong Seung Kim**[1,*]

[1]Department of Chemistry, Korea University, Seoul 02841 Korea

[2]Department of Life Sciences, Korea University, Seoul 02841, Korea

[3]Department of Chemistry, University of Texas at Austin, Austin, Texas 78712-1224, United States

[4]Chuncheon Center, Korea Basic Science Institute, Chuncheon 24341, Korea

[5]These authors contributed equally

[6]Current address: KU Leuven, Rega Institute for Medical Research, Medicinal Chemistry, B-3000 Leuven, Belgium

[7]Lead Contact

SUMMARY

Tumor recurrence as a result of therapy-induced nuclear DNA lesions is a major issue in cancer treatment. Currently, only a few examples of potentially non-genotoxic drugs have been reported. Mitochondrial re-localization of ciprofloxacin, one of the most commonly prescribed synthetic antibiotics, is reported here as a new approach. Conjugating ciprofloxacin to a triphenyl phosphonium group (giving lead Mt-CFX), is used to enhance the concentration of ciprofloxacin in the mitochondria of cancer cells. The localization of Mt-CFX to the mitochondria induces oxidative damage to proteins, mtDNA, and lipids. A large bias in favor of mtDNA damage over

*Correspondence: chi6302@korea.ac.kr (S.-G. Chi), sessler@cm.utexas.edu (J.L.S; lead contact), peter.verwilst@kuleuven.be (P.V.), and jongskim@korea.ac.kr (J.S.K).

AUTHOR CONTRIBUTIONS

Synthesis, characterization and solution experiments: K.S. Biological experiments M.W. and K.-P.K. Statistical analyses: M.W. Writing, review & editing: P.V., K.S., M.W., J.F.A., and J.L.S. Study-enabling funding was provided to: K.S., M.W., S.-G.C., P.V., J.F.A., J.L.S., and J.S.K. Initial project conception: K.S., P.V., and J.S.K. Supervision and project development: S.-G.C., J.L.S., P.V., J.F.A., and J.S.K. All authors proofread, commented on, and approved the final version of the manuscript.

DATA AND SOFTWARE AVAILABILITY

The micro array data was deposited in the NCBI Gene Expression Omnibus (GEO; http://www.ncbi.nlm.nih.gov/geo/) under accession number GSE137679.

SUPPLEMENTAL INFORMATION

The supplemental Information includes experimental procedures, synthetic procedures, and characterization data for of new compounds, as well as 18 supplemental figures (Figures S1-S18), and 2 Tables (Tables S1-S2). The associated files and can be found linked to this article online.

DECLARATION OF INTERESTS

Mt-CFX and analogues as non-genotoxic anticancer agents are the subject of a pending patent application, filed by Korea University, with J.S.K, K.S., P.V. and M.W. named as inventors. J.L.S. holds a part-time summer position at Shanghai University.

nDNA was seen with Mt-CFX, contrary to classic cancer chemotherapeutics. Mt-CFX was found to reduce cancer growth in a xenograft mouse model and proved to be well tolerated. Mitochondrial relocalization of antibiotics could emerge as a useful approach to generating anticancer leads that promote cell death via the selective induction of mitochondrially-mediated oxidative damage.

Graphical Abstract

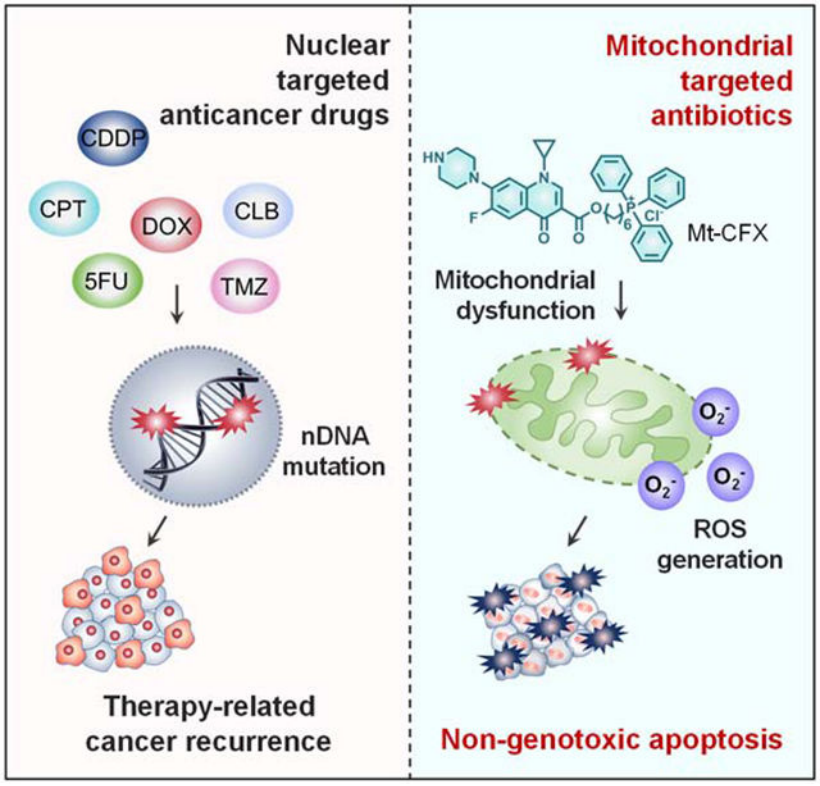

eTOC blurb

Therapy-associated nuclear DNA damage is a key driver for secondary malignancies. It represents a major problem in clinical practice that has yet to be overcome. The mitochondria-targeted ciprofloxacin conjugate reported here eliminates therapy-induced nuclear DNA mutagenicity and induces cancer cell death as the result of oxidative damage. These findings could provide a new framework for the development of non-genotoxic therapeutics that overcome the conceptual limitations of the inherently mutagenic chemotherapeutics that define the current standard of care in cancer chemotherapy.

Keywords

Non-genotoxic cancer therapy; Mitochondria; Targeted therapeutics; Prodrug; DNA damage; Reactive oxygen species; Ciprofloxacin

INTRODUCTION

Tumor recurrence remains the greatest challenge in cancer therapy and is responsible for up to 90% of cancer mortality.[1] Paradoxically, recurrence is often elicited by chemotherapeutics due to the accumulation of nuclear genomic mutations during the treatment regime.[2] Antineoplastic agents relying on direct nuclear DNA damage, such as alkylating agents, are common chemical mutagens and have been implicated in tumor recurrence, e.g., therapy-related acute myeloid leukemia (t-AML).[3–6] Additionally, drug-induced genomic alterations are carried over into the next generation, detectable up to two generations in mice.[7] Given the steady increase in pediatric malignancy survival rates,[8] prevention of these long-term effects might warrant a paradigm shift towards rationally designed non-genotoxic chemotherapeutics.

Mitochondria lie at the nexus of cellular signaling events, including the induction of apoptosis via the caspase cascade. As such, mitochondrial damage-induced programmed cell death represents an appealing pathway for cancer chemotherapy. Agents that target the mitochondria could bypass direct nuclear DNA damage mechanisms, thus preventing the accumulation of nuclear DNA mutations. Mitochondria are widely believed to have a bacterial evolutionary origin and share many similarities with the bacterial genome and biosynthetic machinery.[9] While operating via disparate mechanisms in bacteria and eukaryotic cells, common antibiotics such as fluoroquinolones, aminopenicillins, aminoglycosides ,and tetracyclines inhibit the mitochondrial electron transfer chain (ETC).[10] The associated reduction in mitochondrial electron transfer efficiency leads to the production of ROS,[10] resulting in mitochondrial damage. This damage can trigger apoptosis. We thus thought that by targeting antibiotics to the mitochondria it might be possible to discover new non-genotoxic drugs for cancer chemotherapy. The present study was designed to test this hypothesis.

Efforts to apply antibiotics to cancer chemotherapy have a long history.[11,12] For instance, bacteria-derived bactericides, such as doxorubicin and mitomycin C, have found broad clinical applications in chemotherapy; however, their mode of action is thought to involve direct nuclear DNA damage, which can lead to drug-induced genomic alterations.[13,14] In contrast, many commonly prescribed synthetic bactericidal drugs were developed with a goal of maintaining low toxicity levels in eukaryotic cells. This has made the standard repurposing of such FDA-approved drugs as potential anticancer agents attractive. However, difficulties in achieving effective sub-cellular localization of such antibiotics has, in part, prevented success. While large doses of synthetic antibiotics have been shown to reduce cancer cell viability, typically non-cancerous cells have proved more susceptible to these antimicrobiocidal drugs than cancer cells.[15] Nonetheless, the potential role of antibiotics as chemotherapy adjuvants has been noted.[16] Below, we show that redirection of the antibiotic ciprofloxacin (**CFX**) to the mitochondria via chemical modification results in a new agent with cancer cell selective antiproliferative activity. A reduction *in vivo* is also seen as inferred from tumor regrowth experiments in murine models. The approach illustrated here could overcome the difficulties encountered in the standard repurposing of antibiotics for cancer treatment.

RESULTS AND DISCUSSION

Mt-CFX induces cell death in a mitochondrial membrane potential (MMP)-dependent way

Ciprofloxacin (**CFX**) is one of the most commonly prescribed synthetic antibiotics worldwide. It is thus an attractive target for repurposing as a potential anticancer agent. However, we hypothesized that in order to be effective in this latter regard **CFX** would need to be directed to the mitochondrial. To test this hypothesis, **CFX** was linked to a triphenyl phosphonium subunit, a group known to promote mitochondria localization.[17,18] The resulting conjugate, **Mt-CFX** (Figure 1A; for synthesis, see the Supplemental Information), was found to reduce cell viability in a dose-dependent manner in MDA-MB-231 cancer cells (Figure 1B). An IC_{50} value of 31 μM was recorded for **Mt-CFX,** while **CFX** or the phosphonium targeting group alone proved several orders of magnitude less effective (Figure 1B). An associated BrdU incorporation assay revealed a statistically significant reduction in cell proliferation in the presence of **Mt-CFX** as compared to **CFX** or vehicle only (Figure S1). Relative to MDA-MB-231, a reduced cytotoxicity profile was seen for **Mt-CFX** in the non-cancerous MCF10A mammary gland epithelial cell line (Figure 1C), thus illustrating cancer selectivity *in vitro*. The antiproliferative effect of **Mt-CFX** was found to be on the same order of magnitude across several cancerous cell lines (e.g., MDA-MB-231, SW620, DU145, A549, and PC3). The toxicity of **Mt-CFX** was at least an order of magnitude lower in the normal human fibroblast cell line (BJ) as compared to the cancer cell lines. Moreover, as noted above, virtually no toxicity was observed in the MCF 10A cell line (Figure 1F).

JC-1 monomer/aggregate flow cytometry assays were used in this study to assess the mitochondrial membrane potentials (MMP), with high proportions of monomer fluorescence corresponding to a decreased MMP. The addition of **Mt-CFX** to MDA-MB-231 cells resulted in a time-dependent MMP depolarization (Figures 1D and S2) with a concurrent increase in Annexin-V binding (Figures 1E and S3). Such findings are consistent with an apoptosis-induced cell death mechanism. We thus sought to investigate the relationship, if any, between cell viability and the mitochondrial membrane potential. A population of each cell line was subjected to a JC-1 assay (Figures 1G and S4). A strong general trend towards lower cell viability with stronger MMP hyperpolarization was found (Figure 1H).

Localization of the Mt-CFX system to the mitochondria as evidenced by studies of a fluorescent probe, Bo-Mt-CFX

To obtain further support for the suggestion that **Mt-CFX** localizes to the mitochondria, we synthesized a related conjugate incorporating the fluorophore resorufin. This system, termed **Bo-Mt-CFX**, was designed to allow for an accurate spatiotemporal analysis of the drug action *in vitro* and *in vivo* (see the Supplemental Information for synthetic details).[19–22] A phenylboronate moiety was used to prepare **Bo-Mt-CFX** since it is a known trigger that will undergo peroxide-induced cleavage, thus allowing release of both the fluorophore and putative **Mt-CFX** drug under conditions of ROS over-production (i.e., in cancerous tissues).[23] As can be seen in Figure 2A, peroxide-triggered drug release results in the liberation of the CFX and the fluorophore resorufin. This self-immolative release relies on the formation

and subsequent nucleophilic attack of various quinone methide moieties which are produced throughout the release mechanism.

We validated the peroxide-triggered self-immolative release of the resorufin fluorophore from **Bo-Mt-CFX** in aqueous solution (5 μM) by observing the characteristic fluorescent band centered at 580 nm. We observed a clear time-dependent response with a half-life of approximately 6,000 s in the presence of 50 equiv. of H_2O_2 (Figure S5A). A concentration-dependent effect was also observed (Figure S5B). Moreover, the identity of the fluorescent species was confirmed to be resorufin via a time-dependent HPLC assay. On this basis, we conclude that under these test conditions the self-immolative reaction is complete within 8 hours (Figure S6). **Mt-CFX** release was also confirmed by HPLC/MS (Figure S7). The influence of **Bo-Mt-CFX** on intracellular cellular ROS and its effects on cellular activity (i.e., cell viability across a panel cell lines, glutathione homeostasis, ROS dependence) was further evaluated *in vitro* (Figures S8–S14), revealing the expected correlation between cancer cell inhibition and cellular oxidative stress.

Confocal microscopy studies confirmed that in MDA-MB-231 cells release of resorufin from **Bo-Mt-CFX** occurs in the mitochondria (Figure 2B). The **Mt-CFX** released from **Bo-Mt-CFX** was found to be largely retained in the mitochondria for at least 8 hours (Figure S15). The addition of **Bo-Mt-CFX** to MDA-MB-231 cells also resulted in the activation of the caspase pathway (Figures 2C and S16), while engendering a dose-dependent cytoplasmic relocalization of cytochrome *c* (Figures 2D and S16). An in-depth study of several pro-apoptotic (BAX, BAC, BAD, PUMA, Noxa, and BID) and anti-apoptotic (Bcl-2, Bcl-w, Mcl-1, Bcl-xl and A1) members of the Bcl-2 family was conducted in the presence of **Mt-CFX** (Figure S17). A lowered or constant protein expression level was found for the anti-apoptotic proteins, while the pro-apoptotic BAX levels were increased. The PUMA and Noxa levels were scarcely elevated, which is consistent with a lack of (nuclear) genotoxicity.[24] Finally, a comparison between Mt-HCT116 WT and HCT116 $Bax^{-/-}$ cells revealed the requirement of BAX for apoptosis induction following **Mt-CFX** treatment (Figure S18), a finding that supports mitochondrial involvement in the cell death process. Taken together, these results lead us to conclude that the activity of **Mt-CFX** is strongly dependent on the mitochondrial accumulation of the drug, a phenomenon that generally tracks with the MMP.

Mt-CFX induces mitochondrial ROS production with minimal nuclear DNA damage

Several antibacterial drugs have been reported to cause mitochondrial damage as a result of ROS production.[10] Therefore, we investigated the influence of **Mt-CFX** on ROS production in MDA-MB-231 cells. As can be seen in Figure 3A, the intracellular Amplex red fluorescence was elevated in cells treated with **Mt-CFX** and this indicator. The fluorescence intensity ascribed to Mito-SOX, a mitochondria-selective superoxide ($O_2^{\bullet -}$) fluorescent dye, is likewise enhanced upon treatment with **Mt-CFX**. Such findings are consistent with an increase in ROS production within the mitochondria (Figures 3B and S19A). The use of the non-selective fluorescein-based oxidative stress indicator, CM-H2DCFDA, provided further support for the contention that ROS are being generated in the presence of **Mt-CFX** (cf. Figures 3C and S19B). Furthermore, cells pre-incubated with *N*-acetyl cysteine (NAC) (cf.

Figures S20–S21) or other antioxidants (Figure S21) not only decreased the cellular ROS burden but rescued cells from **Mt-CFX**-induced cytotoxicity.

We next investigated whether damage to cellular components ascribable to ROS was seen upon incubation of MDA-MB-231 cells with **Mt-CFX** or **CFX** (Figure 3D and Figure S22). We found elevated 8-hydroxy-2′-deoxyguanosine (8-OHdG) levels, a classic marker for radical-induced oxidative damage to nuclear and mitochondrial DNA. Both protein carbonylation and elevated malondialdehyde (MDA) levels were seen. These are indicators of protein oxidation and lipid peroxidation, respectively. Thus, considered in concert, these results lead us to suggest that **Mt-CFX** interferes with the mitochondrial ETC process, inducing a significantly enhanced level of oxidative stress. TEM (transmission electron microscopy) revealed noticeable morphology changes, including the loss of cristae, deformation and mitochondrial swelling, when treated with **Mt-CFX** alone, while NAC pre-treatment also prevented discernable mitochondrial damage (Figure S23). Mitochondrial de-energization was found to mirror these observations, as the cellular ATP content was reduced in the case of **Mt-CFX** treated cells, but not for those pre-treated with NAC (Figure S24)

The nature and extent of **Mt-CFX**-mediated DNA was then explored. Oxidative DNA damage induces the expression of base-excision repair proteins in both the nucleus and mitochondria, whereas nucleotide-excision repair (NER) expression is localized to the nucleus.[25] We thus employed quantitative PCR (q-PCR) to probe the expression levels of organelle-specific repair enzymes upon **Mt-CFX** treatment. Doxorubicin (**DOX**) was also studied since this clinically approved drug is known to induce ROS production.[8] *POLG*, encoding a mitochondria-selective base excision repair protein, was found to be significantly increased following incubation with **Mt-CFX** only (Figure 3E). **DOX**, on the other hand, elicited a clear upregulation of NER, as observed for both *ERCC1* and *DDB2*, while **Mt-CFX** did not cause significantly increased expression levels. Under these conditions treatment with **CFX** alone did not lead to an upregulation in any of these repair enzymes.

The impact of **Mt-CFX** on cellular protein metabolism was investigated by monitoring the expression levels of a nuclear (*GAPDH*, glyceraldehyde 3-phosphate dehydrogenase) and mitochondrial (ND_1, NADH-ubiquinone oxidoreductase chain 1) housekeeping proteins. While **DOX** treatment produced a reduction in *GAPDH* expression levels, no statistically alterations in *GAPDH* were seen upon exposure to either **Mt-CFX** or **CFX**. Conversely, **Mt-CFX** was found to interfere with mitochondrial function (Figure 3F). Furthermore, **Mt-CFX** was found to reduce the *ND1/GAPDH* expression level ratio in both a dose- and time-dependent manner. On the other hand, a much smaller reduction in the mitochondrial/nuclear expression level ratio was observed for **CFX** (Figure S25).

The extent of drug-induced mitochondrial DNA mutation was then measured using a *TaqI* restriction site mutation assay.[26] This restriction enzyme cleaves the double stranded 5′-TCGA-3′ DNA sequence leading to DNA digestion. In contrast, restriction enzyme-resistant sites undergo PCR amplification. **Mt-CFX**-treated cells showed an approximately 4.5-fold increase in resistance to *TaqI* restriction, whereas no significant difference in the amount of *TaqI* resistance was observed in the case of DOX-treated cells (Figure 3G).

We also investigated the location of predominant DNA mutagenicity for **Mt-CFX**, as well as that for several conventional chemotherapeutic drugs, including doxorubicin (**DOX**), temozolomide (**TMZ**), camptothecin (**CPT**), *cis*-platin (**CDDP**), chlorambucil (**CLB**), and fluorouracil (**5-FU**). Long range qPCR (3129 bp and 3723 bp for nuclear and mitochondrial targets, respectively)[27] revealed that all the conventional drugs induced a considerable amount of nuclear DNA mutations, while having relatively little effect on the mitochondrial genome. In contrast, **Mt-CFX** was found to promote mitochondrial DNA damage while engendering little in the way of nuclear DNA damage (Fig 3H). This mirrors the lack of increase in the PUMA and Noxa protein levels (cf. Figure S17). Taken in aggregate, these results are consistent with our core hypothesis, namely that **Mt-CFX** localizes to the mitochondria and induces levels of ROS that are increased to the point where mitochondrial (but not nuclear) DNA damage is seen.

Identification of cellular processes affected by Mt-CFX

A DNA microarray study, comprising 197 genes, was conducted to determine the impact of **Mt-CFX** on protein expression and pathway activation in MDA-MB-231 cells (Figure 4A,B). Several pathways related to programmed cell death, such as apoptosis, ferroptosis and necroptosis, were altered in a statistically significant manner. Genes corresponding to the biosynthesis and metabolism of amino acids, fatty acids, and pyruvate were also affected.

Selected examples of gene expression levels were assayed using q-PCR (Figure 4C). On this basis it is inferred that cellular metabolism is strongly affected by **Mt-CFX**, as reflected in an increased expression of the transaminase, pyruvate synthesis, and folate metabolism pathways (*GPT2*, *ME1* and *MTHFD2*). Importantly, we also found that several ROS-induced cellular responses were upregulated in the presence of **Mt-CFX**. A mitochondrial aldehyde dehydrogenase (*ALDH2*) gene was significantly overexpressed. Presumably, this overexpression reflects a need to mitigate the effects of increased protein carbonylation, which is a recognized form of ROS damage (Figure 4D). *GADD45A*, encoding for a protein involved in stimulating DNA excision repair and inducing cell cycle arrest, was also overexpressed by ~12-fold (Figure 4E). An approximately 20-fold overexpression of *NLRP1* was also seen, which is taken as evidence of cellular structure damage and the induction of the *NLRP1* inflammasome (Figure 4E). *DDIT4* and *SESN2*, involved in inhibiting mTORC1 and thus enabling autophagy, were overexpressed by ~40-fold and ~23-fold, respectively, indicating a need for the degradation of damaged cellular components. Overexpression of *MAP1LC3B* was also detected; this result suggests that damaged mitochondria are being degraded via mitophagy and may indicate onset of ferroptosis (Figure 4F).

In vivo tumor growth reduction by Mt-CFX and Bo-Mt-CFX

Finally, we investigated the *in vivo* activity of **Mt-CFX** in MDA-MB-231 tumor xenograft-bearing mice. All agents (e.g., vehicle, **CFX**, **Mt-CFX**, and **Bo-Mt-CFX**) were administered intravenously to these mice via tail vein injection. To assess biolocalization *in vivo*, **Bo-Mt-CFX** was administered to mice and its fluorescence was monitored. Fluorescence was detected at the tumor site and was found to persist >48 hours (Figure 5A). We confirmed that the inferred selectivity was indeed cancer specific by *ex vivo* analyses of organs harvested

from mice euthanized 48 hours after a single **Bo-Mt-CFX** treatment. Nearly all fluorescence was confined to the tumor site, whereas other organs, such as the heart and reticuloendothelial system, remained unaffected (Figure 5B).

Chemotherapeutic intervention was investigated using a 3-week regimen involving 1-dose per week treatment with 5 mmol kg^{-1} **CFX**, **Mt-CFX**, **Bo-Mt-CFX**, or vehicle alone. The study revealed a statistically significantly reduction in tumor growth in mice treated with **Bo-Mt-CFX** or **Mt-CFX** from the sixth week onwards (Figure 5C). The experiment was terminated at the twelfth week, when the tumors in the control group reached 1,000 mm^3. The reduction in tumor burden produced by **Bo-Mt-CFX** or **Mt-CFX** was mirrored in the excised tumor weights (Figure 5E,F). This treatment regime was well-tolerated by the mice and no significant differences in animal body weights were observed during the course of treatment (Figure 5D). Liver function tests at the experimental endpoint revealed no significant differences relative to the outset, with the overall AST and ALT ratios of all mice being within the normal range.[28]

Tissue samples from the 4 treatment groups were subjected to immunohistochemistry. Cells with cleaved caspase were clearly more prevalent in the **Mt-CFX** and **Bo-Mt-CFX** groups, while a Ki-67 cell proliferation also revealed a dramatic reduction in cell proliferation in these two treatment groups (Figure 5E). Finally, tissue samples from tumor, liver, heart, spleen and kidneys were subject to H & E (haemotoxylin and eosin) staining. These studies revealed statistically significant differences in the histology for the tumor samples obtained from the mice treated with **Mt-CFX** or **Bo-Mt-CFX** relative to controls. Importantly no obvious signs of tissue damage were found in any of the other samples subject to analysis (Figure 5E).

CONCLUSION

Based on the findings presented here, we propose that **Mt-CFX** acts as a mitochondrially targeted chemotherapeutic drug. **Mt-CFX** was found to have inherent selectivity towards cancer cells. The use of the fluorescent conjugate **Bo-Mt-CFX** revealed mitochondrial localization, whereas an oxidative stress response was seen when MDA-MB-231 cells were treated with either **Mt-CFX** system. **Mt-CFX** was found to interfere with the mitochondrial ETC, inducing significantly enhanced levels of ROS. This was reflected in increased protein carbonylation, lipid peroxidation, and oxidative DNA damage *in vitro*. Moreover, **Mt-CFX** was found to cause a dramatic decrease in nuclear DNA damage as compared to **DOX**, **TMZ**, **CPT**, **CDDP**, **CLB** and **5-FU**. **Bo-Mt-CFX** was retained in tumor xenografts as inferred from fluorescent imaging, while treatment of xenograft-bearing mice with well-supported doses of **Mt-CFX** and **Bo-Mt-CFX** resulted in reduced cancer burden. We thus suggest that rerouting **CFX** and potentially other approved antibiotics to the mitochondria could provide a new approach to generating small molecule chemotherapeutics. Support for this notion comes from the finding that the present system appears to be free of many of the genotypic-based side-effects that plague the majority of chemotherapeutics in current use.

EXPERIMENTAL PROCEDURES

The full experimental procedures are provided in the Supplemental Information.

Supplementary Material

Refer to Web version on PubMed Central for supplementary material.

ACKNOWLEDGMENTS

This work was supported by the National Research Foundation of Korea (NRF) funded by the Ministry of Science and ICT (2018R1A2A1A05020236, S.-G.C. and CRI project no. 2018R1A3B1052702, J.S.K.) and the Basic Science Research Program (2017R1D1A1B03032561, P.V. and 2017R1D1A1B03030062, M.W.) funded by the Ministry of Education as well as the Korea Research Fellowship Program funded by the Ministry of Science and ICT through the National Research Foundation of Korea (2016H1D3A1938052, P.V.). K.S. is a recipient of the global PhD fellowship (GPF) program of the NRF funded by the Ministry of Science and ICT, Korea (2014H1A2A1020978, K.S.). Funding from the National Cancer Institute (RO1 CA68682 for J.L.S. and R15 CA232765 for J.F.A.) is acknowledged.

REFERENCES AND NOTES

1. Mehlen P, and Puisieux A (2006) Metastasis: a question of life or death. Nat. Rev. Cancer 6, 449–458. [PubMed: 16723991]
2. Grosse Y, Baan R, Straif K, Secretan B, El Ghissassi F, Bouvard V, Benbrahim-Tallaa L, Guha N, Galichet L, and Cogliano V (2009) A review of human carcinogens—Part A: pharmaceuticals. Lancet Oncol. 10, 13–14. [PubMed: 19115512]
3. Eichenauer DA, Thielen I, Haverkamp H, Franklin J, Behringer K, Halbsguth T, Klimm B, Diehl V, Sasse S, Rothe A, et al. (2014) Therapy-related acute myeloid leukemia and myelodysplastic syndromes in patients with Hodgkin lymphoma: a report from the German Hodgkin Study Group. Blood 123, 1658–1664. [PubMed: 24478403]
4. Pui CH, Ribeiro RC, Hancock ML, Rivera GK, Evans WE, Raimondi SC, Head DR, Behm FG, Mahmoud MH, Sandlund JT, et al. (1991) Acute Myeloid-Leukemia in Children Treated with Epipodophyllotoxins for Acute Lymphoblastic-Leukemia. New Engl. J. Med 325, 1682–1687. [PubMed: 1944468]
5. Travis LB, Holowaty EJ, Bergfeldt K, Lynch CF, Kohler BA, Wiklund T, Curtis RE, Hall P, Andersson M, Pukkala E, et al. (1999) Risk of leukemia after platinum-based chemotherapy for ovarian cancer. New Engl. J. Med 340, 351–357. [PubMed: 9929525]
6. Bhatia S, Robison LL, Oberlin O, Greenberg M, Bunin G, Fossati-Bellani F, and Meadows AT (1996) Breast cancer and other second neo-plasms after childhood Hodgkin's disease. New Engl. J. Med 334, 745–751. [PubMed: 8592547]
7. Glen CD, and Dubrova YE (2012) Exposure to anticancer drugs can result in transgenerational genomic instability in mice. P. Natl. Acad. Sci. USA 109, 2984–2988
8. Smith MA, Seibel NL, Altekruse SF, Ries LAG, Melbert DL, O'Leary M, Smith FO, and Reaman GH (2010) Outcomes for Children and Adolescents With Cancer: Challenges for the Twenty-First Century. J. Clin. Oncol 28, 2625–2634. [PubMed: 20404250]
9. Dyall SD, Brown MT, and Johnson PJ (2004) Ancient invasions: From endosymbionts to organelles. Science 304, 253–257. [PubMed: 15073369]
10. Kalghatgi S, Spina CS, Costello JC, Liesa M, Morones-Ramirez JR, Slomovic S, Molina A, Shirihai OS, and Collins JJ (2013) Bactericidal Antibiotics Induce Mitochondrial Dysfunction and Oxidative Damage in Mammalian Cells. Sci. Transl. Med 5, 192ra85.
11. DeVita VT Jr., and Chu E (2008) A History of Cancer Chemotherapy. Cancer Res. 68, 8643–8653. [PubMed: 18974103]
12. Galm U, Hager MH, Van Lanen SG, Ju J, Thorson JS, and Shen B (2005) Antitumor Antibiotics: Bleomycin, Enediynes, and Mitomycin. Chem. Rev 105, 739–758. [PubMed: 15700963]

13. Tacar O, Sriamornsak P, and Dass CR (2013) Doxorubicin: an update on anti-cancer molecular action, toxicity and novel drug delivery systems. J. Pharm. Pharmacol 65, 157–170. [PubMed: 23278683]
14. Fu D, Calvo JA, and Samson LD (2012) Balancing repair and tolerance of DNA damage caused by alkylating agents. Nat. Rev. Cancer 12, 104–120. [PubMed: 22237395]
15. Esner M, Graifer D, Lleonart ME and Lyakhovich A (2017) Targeting cancer cells through antibiotics-induced mitochondrial dysfunction requires autophagy inhibition. Cancer Lett. 384, 60–69. [PubMed: 27693455]
16. Alibek K, Bekmurzayeva A, Mussabekova A, and Sultankulov B (2012) Using antimicrobial adjuvant therapy in cancer treatment: a review. Infect. Agent Cancer 7, 33. [PubMed: 23164412]
17. Zielonka J, Joseph J, Sikora A, Hardy M, Ouari O, Vasquez-Vivar J, Cheng G, Lopez M, and Kalyanaraman B (2017) Mitochondria-Targeted Triphenylphosphonium-Based Compounds: Syntheses, Mechanisms of Action, and Therapeutic and Diagnostic Applications. Chem. Rev 117, 10043–10120. [PubMed: 28654243]
18. Samanta S, He Y, Sharma A, Kim J, Pan WH, Yang ZG, Li J, Yan W, Liu LW, Qu JL, and Kim JS (2019) Fluorescent Probes for Nanoscopic Imaging of Mitochondria. Chem 5, 1697–1726.
19. Lee MH, Sharma A, Chang MJ, Lee J, Son S, Sessler JL, Kang C and Kim JS (2018) Fluorogenic reaction-based prodrug conjugates as targeted cancer theranostics. Chem. Soc. Rev 47, 28–52. [PubMed: 29057403]
20. Zhang R, Xu Y, Zhang Y, Kim HS, Sharma A, Gao J, Yang G, Kim JS and Sun Y (2019) Rational design of a multifunctional molecular dye for dual-modal NIR-II/photoacoustic imaging and photothermal therapy. Chem. Sci 10, 8348–8353. [PubMed: 31803412]
21. Sun Y, Ding F, Zhou Z, Li C, Pu M, Xu Y, Zhan Y, Lu X, Li H, Yang G, et al. (2019) Rhomboidal Pt(II) metallacycle-based NIR-II theranostic nanoprobe for tumor diagnosis and image-guided therapy. Proc. Natl. Acad. Sci. USA 116, 1968–1973. [PubMed: 30670648]
22. Sun Y, Ding F, Chen Z, Zhang R, Li C, Xu Y, Zhang Y, Ni R, Li X, Yang G, et al. (2019) Melanin-dot-mediated delivery of metallacycle for NIR-II/photoacoustic dual-modal imaging-guided chemo-photothermal synergistic therapy. Proc. Natl. Acad. Sci. USA 116, 16729–16735. [PubMed: 31391305]
23. Liou GY, and Storz P (2010) Reactive oxygen species in cancer. Free Radical Res. 44, 479–496. [PubMed: 20370557]
24. Yu J, and Zhang L (2008) PUMA, a potent killer with or without p53. Oncogene 27, S71–S83. [PubMed: 19641508]
25. Dianov GL, Souza-Pinto N, Nyaga SG, Thybo T, Stevnsner T, and Bohr VA (2001) Base excision repair in nuclear and mitochondrial DNA. Prog. Nucleic Acid Res. Mol. Biol 68, 285–297. [PubMed: 11554304]
26. Vermulst M, Bielas JH, and Loeb LA (2008) Quantification of random mutations in the mitochondrial genome. Methods 46, 263–268. [PubMed: 18948200]
27. Evans SO, Jameson MB, Cursons RT, Peters LM, Bird S, and Jacobson GM (2016) Development of a qPCR Method to Measure Mitochondrial and Genomic DNA Damage with Application to Chemotherapy-Induced DNA Damage and Cryopreserved Cells. Biology (Basel) 5, 39–49.
28. Sher Y and Hung M (2013) Blood AST, ALT and UREA/BUN Level Analysis. Bio-protocol 3, e931.

The Bigger Picture

Cancer recurrence is a major concern in clinical practice, severely limiting the life expectancy of cancer patients. Recurrence is often the result of therapy, which can also lead to drug-induced secondary tumorigenesis. In many cases, the resulting secondary malignancies are the result of nuclear DNA lesions induced by traditional genotoxic chemotherapeutics. In this study we show that by rerouting a commonly used microbiocidal, ciprofloxacin, to the mitochondria, it is possible to produce a highly selective and well-tolerated anticancer agent. Mitochondrial targeting not only induces a high degree of cancer specificity, it also minimizes nuclear DNA damage. On the other hand, it promotes mitochondrial damage-associated cancer cell death and tumor growth reduction. The present targeted ciprofloxacin derivative thus illustrates what could emerge as a new approach to generating less genotoxic and more effective chemotherapeutics.

Highlights

- Mitochondrial re-localization of ciprofloxacin reduces nuclear genotoxicity
- Mitochondrial localization and spatiotemporal drug activation were confirmed
- qPCR analyses provide support for the proposed mode of action
- *In vivo* experiments support the efficacy and target-specificity

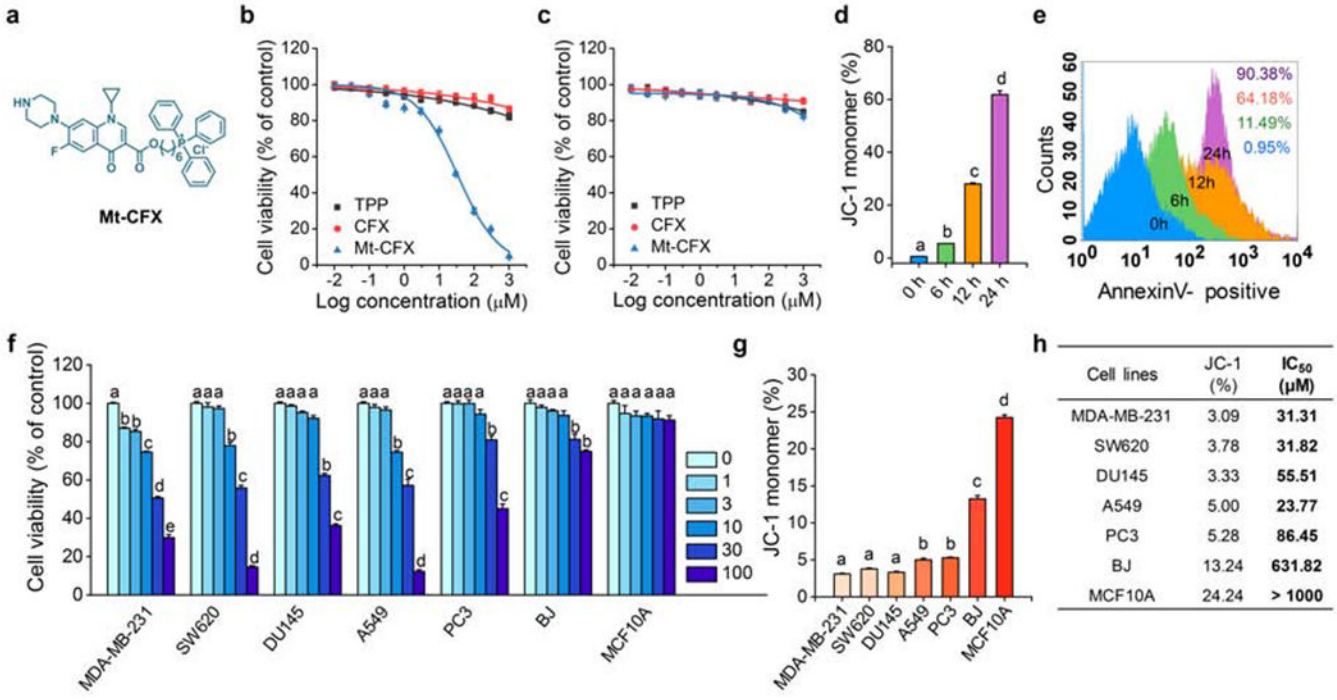

Cell lines	JC-1 (%)	IC_{50} (μM)
MDA-MB-231	3.09	**31.31**
SW620	3.78	**31.82**
DU145	3.33	**55.51**
A549	5.00	**23.77**
PC3	5.28	**86.45**
BJ	13.24	**631.82**
MCF10A	24.24	**> 1000**

Figure 1. Mt-CFX induces cell death in a mitochondrial membrane potential (MMP)-dependent manner

(A) Chemical structure of **Mt-CFX**.

(B) Concentration-dependent cell-viability of MDA-MB-231 cells incubated with **Mt-CFX**, **CFX**, and **TPP**, as determined by a Cyto-Tox96 Assay (72h).

(C) Concentration-dependent cell-viability of MCF10A cells incubated with **Mt-CFX**, **CFX**, and **TPP**, as determined by a CytoTox96 Assay (72h).

(D) Proportion of JC-1 monomer fluorescence in a flow cytometry assay of MDA-MB-231 pretreated with 30 μM **Mt-CFX** with incubation times as indicated in the figure.*

(E) Time depended Annexin V-FITC flow cytometry analysis of MDA-MB-231 pretreated with 30 μM **Mt-CFX** per the incubation times indicated in the figure.

(F) Concentration-dependent cell-viability of different cell lines incubated with **Mt-CFX**, as indicated in the figure, as determined by a CytoTox96 Assay (72h).*

(G) Different proportions of JC-1 monomer fluorescence in a flow cytometry assay of untreated cells.

(H) Summarized JC-1 monomer fractions from panel G and IC_{50} values of **Mt-CFX**-treated cell lines from panel F.*

All cytotoxicity experiments were carried out three times and in triplicate wells. Data are represented as mean ± SEM. Statistical significance was determined using a one-way ANOVA test with post-hoc Bonferroni test.

*Different letters (e.g., a–d) signify data which are statistically different ($p < 0.05$).

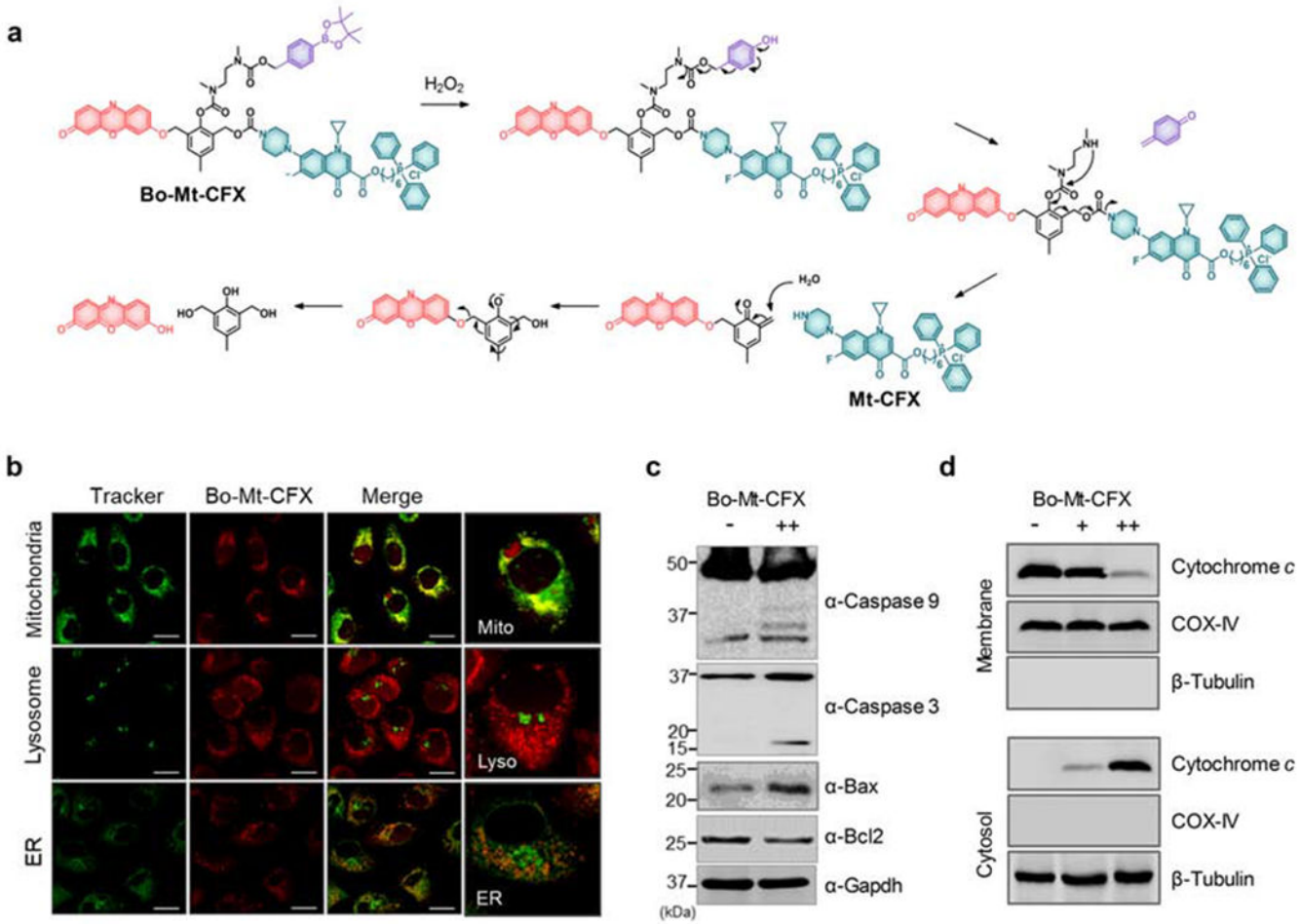

Figure 2. Bo-Mt-CFX, a ROS-triggered DDS system incorporating Mt-CFX

(A) Peroxide-induced self-immolative activation mechanism of **Bo-Mt-CFX**

(B) Localization of resorufin release from 10 μM **Bo-Mt-CFX** in MDA-MB-231 cells, compared with MitoTracker Green FM, LysoTracker Green DND-26, and ER-Tracker Green.

(C) Western blotting of apoptosis-related proteins in MDA-MB-231 cells treated with 10 μM **Bo-Mt-CFX** or a control.

(D) Western blotting of cytochrome c release from mitochondria to the cytosol seen in MDA-MB-231 cells treated with 3 μM or 10 μM **Bo-Mt-CFX**, as well as a control.

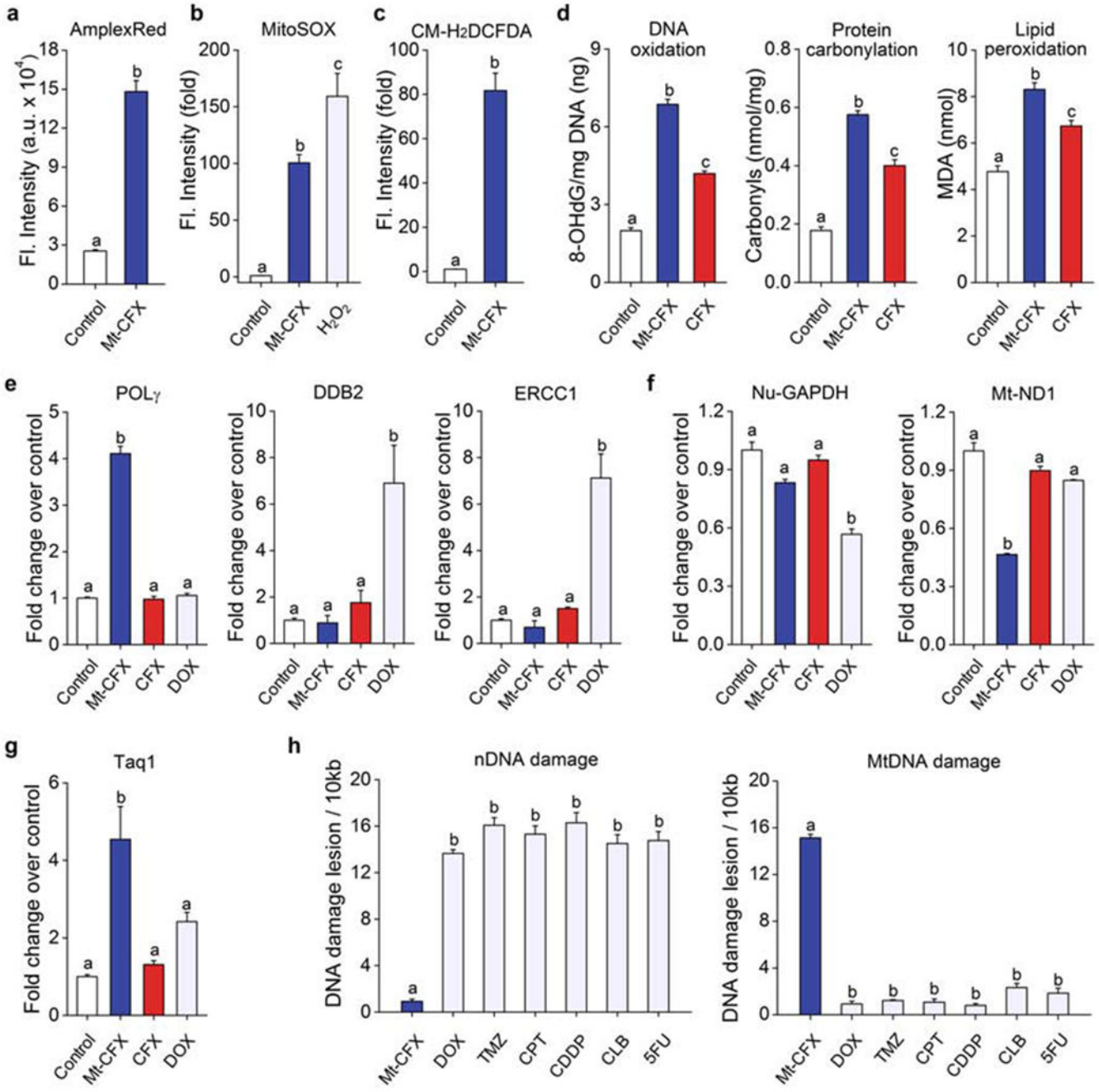

Figure 3. Mt-CFX induces mitochondrial ROS production with minimal nuclear DNA damage

(A) Confocal microscopic fluorescence intensity of MDA-MB-231 cells treated with **Mt-CFX** (30 μM) or a control co-incubated with 400 μM Amplex Red® for 30 min ($n = 6$).

(B) Confocal microscopic fluorescence intensity of **Mt-CFX** (30 μM) or control-treated MDA-MB-231 cells incubated with 5 μM Mito-Sox for 15 min ($n = 5$).

(C) Confocal microscopic fluorescence intensity of **Mt-CFX** (30 μM) or control treated MDA-MB-231 cells incubated with 10 μM CM-H2DCFDA for 30 min ($n = 15$).

(D) ELISA DNA oxidation and protein carbonylation assay results of MDA-MB-231 cells treated with 30 μM **Mt-CFX**, **CFX** as well as control samples. Colorimetric

malondialdehyde (MDA) assay results, as a measure of lipid peroxidation, of similarly treated MDA-MB-231 cells.

(E) q-PCR analysis of DNA repair genes in MDA-MB-231 cells treated with 30 μM **Mt-CFX**, **CFX**, **DOX**, and control samples.

(F) q-PCR analysis of housekeeping genes in MDA-MB-231 cells treated with 30 μM **Mt-CFX**, **CFX**, **DOX**, and control samples.

(G) *Taq1* restriction site mutation assay using MDA-MB-231 cells treated with 30 μM **Mt-CFX**, **CFX**, **DOX**, and control samples.

(H) Long-range q-PCR DNA lesion assay using MDA-MB-231 cells treated with **Mt-CFX** (30 μM), temozolomide (**TMZ**) (1 μM), camptothecin (**CPT**) (250 nM), cis-platin (**CDDP**) (3 μM), chlorambucil (**CLB**) (50 μM), and fluorouracil (**5-FU**) (30 μM), respectively. Concentrations were selected on the basis of their respective IC_{50} values.

Data are represented as mean ± SEM. ($n = 3$, unless specified otherwise). Statistical significance was determined using a one-way ANOVA test with post-hoc Bonferroni test. Different letters (e.g., a–d) signify data which are statistically different ($p < 0.05$).

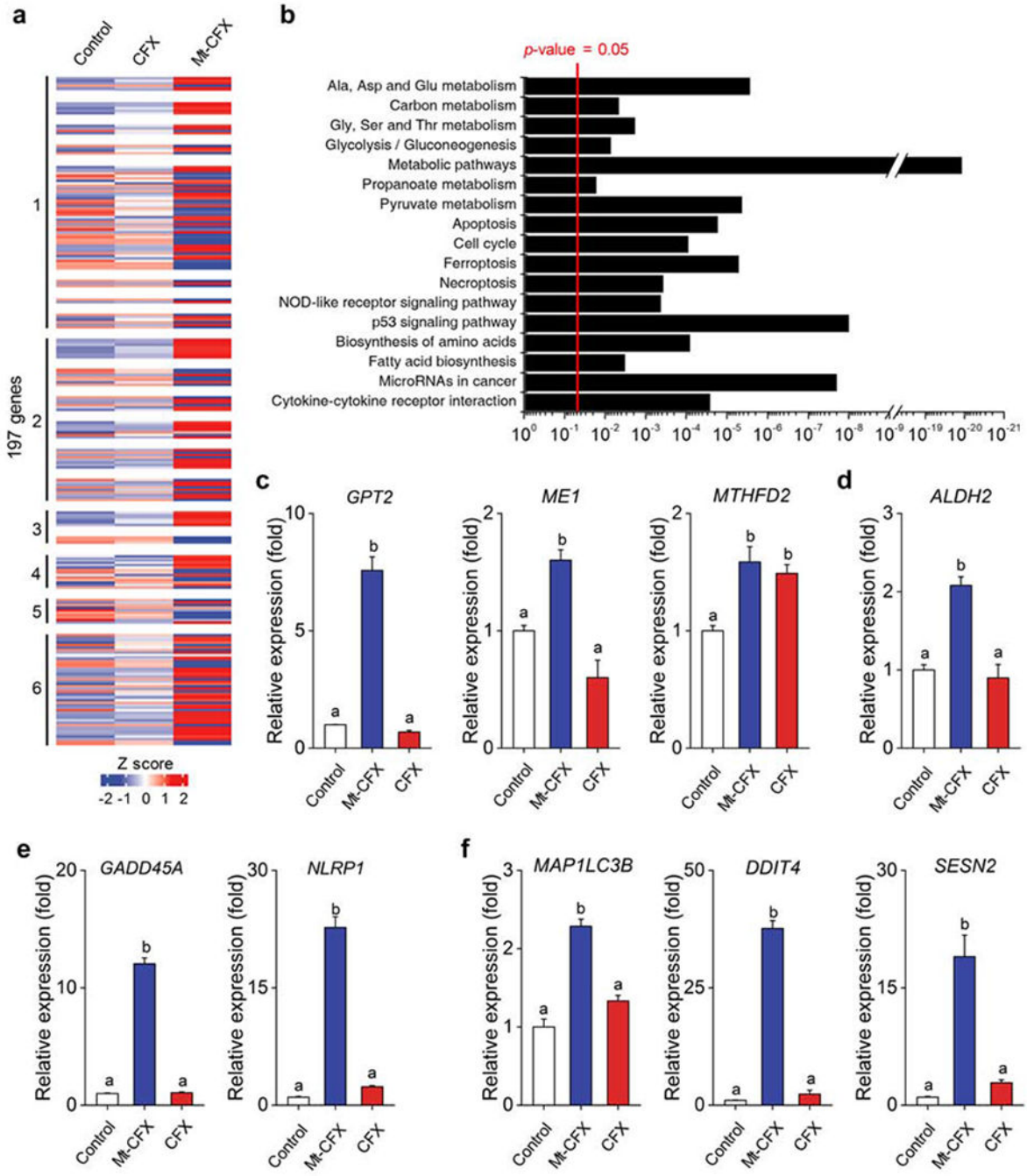

Figure 4. Identification of cellular processes affected by Mt-CFX

(A) Heatmap representing relative expression levels of the DEGs (differentially expressed genes) to control versus 10 μM **CFX** and **Mt-CFX**.

(B) KEGG pathway enrichment analysis of the 197 DEGs.

(C-F) q-PCR gene expression levels of selected genes in cells MDA-MB-231 cells treated with 10 μM **Mt-CFX**, **CFX** and a control sample.

(C) Cellular metabolism.*

(D) Mitochondrial detoxification.*

(E) Cellular repair and inflammasome induction.*

(F) Autophagy and mitophagy.*

Data are represented as mean ± SEM. (n = 3, in panels C-F). Statistical significance in panels c-f was determined using a one-way ANOVA test with post-hoc Bonferroni test. *Different letters (e.g., a–d) signify data which are statistically different ($p < 0.05$).

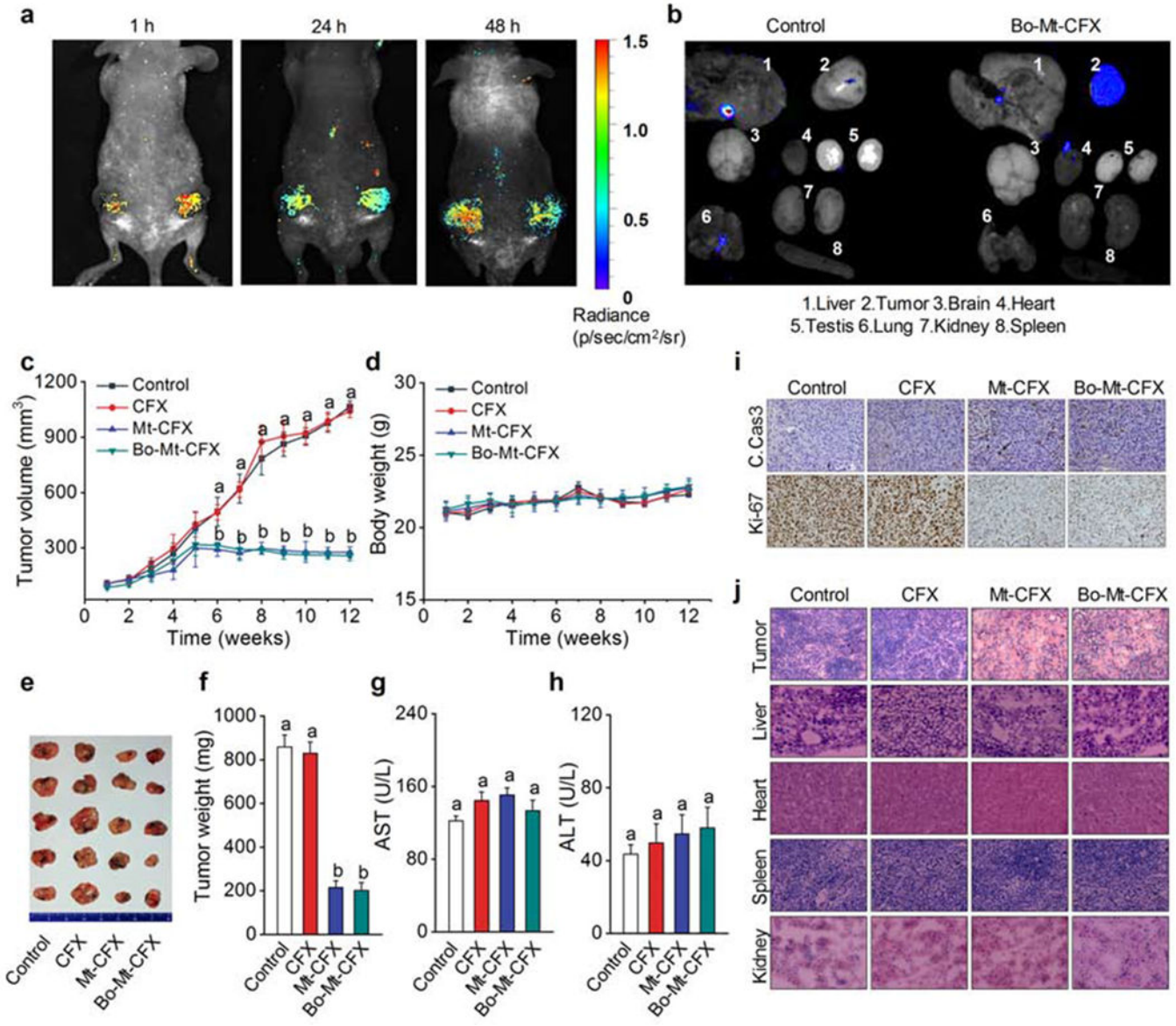

Figure 5. ***In vivo*** **tumor growth reduction by Mt-CFX and Bo-Mt-CFX.**

(A) *In vivo* images of MDA-MB-231 xenograft mouse 1 h, 24 h, and 48 h post intravenous tail vein injection of a single dose of 0.5 μmol kg^{-1} **Bo-Mt-CFX**. Excitation at 550 nm. Emission at 650 nm.

(B) *Ex vivo* imaging of excised tumors and organs 48 h post injection of a single dose of 0.5 μmol kg^{-1} **Bo-Mt-CFX** or vehicle only. Excitation at 550 nm. Emission at 650 nm.

(C) *In vivo* tumor volume determination (1/2 × length × width^2) of mice treated with 0.5 μmol kg^{-1} **CFX**, **Mt-CFX**, **Bo-Mt-CFX**, or vehicle alone, once a week for 3 weeks.*

(D) Body weight of mice during the treatment regime.

(E) Excised tumors at the treatment endpoint.

(F) Excised tumor weight per treatment group.*

(G-H) Blood serum AST and ALT activity levels, as determined using a colorimetric assay.*

(I) Immunohistochemistry (cleaved caspase 3 and Ki-67) of representative tumor tissue slices of the different treatment groups.
(J) H&E staining of representative tissue slices of the different treatment groups.
Data are represented as mean ± SEM. Panels C, D, F: $n = 4$ mice and $n = 8$ tumors per group, Panels G, H: $n = 4$. Statistical significance was determined using a one-way ANOVA test with post-hoc Bonferroni test.
*Different letters (e.g., a–d) signify data sets that are statistically different ($p < 0.05$).